

Characterization of domain wall–based traps for magnetic beads separation

M. Donolato, F. Lofink, S. Hankemeier, J. M. Porro, H. P. Oepen et al.

Citation: *J. Appl. Phys.* **111**, 07B336 (2012); doi: 10.1063/1.3689009

View online: <http://dx.doi.org/10.1063/1.3689009>

View Table of Contents: <http://jap.aip.org/resource/1/JAPIAU/v111/i7>

Published by the [American Institute of Physics](#).

Additional information on J. Appl. Phys.

Journal Homepage: <http://jap.aip.org/>

Journal Information: http://jap.aip.org/about/about_the_journal

Top downloads: http://jap.aip.org/features/most_downloaded

Information for Authors: <http://jap.aip.org/authors>

ADVERTISEMENT



AIPAdvances

Now Indexed in Thomson Reuters Databases

Explore AIP's open access journal:

- Rapid publication
- Article-level metrics
- Post-publication rating and commenting

Characterization of domain wall–based traps for magnetic beads separation

M. Donolato,^{1,a)} F. Lofink,² S. Hankemeier,² J. M. Porro,¹ H. P. Oepen,^{2,3} and P. Vavassori^{1,3}

¹*CIC nanoGUNE Consolider, Tolosa Hiribidea 76, San Sebastian 20009, Spain*

²*Institut für Angewandte Physik, Universität Hamburg, Jungiusstr. 11, Hamburg 20355, Germany*

³*IKERBASQUE, Basque Foundation for Science, Bilbao 48011, Spain*

(Presented 3 November 2011; received 23 September 2011; accepted 24 November 2011; published online 14 March 2012)

We characterize the magnetic behavior of an array of magnetic bead traps based on domain walls (DWs) formed in zig-zag permalloy wires patterned on a Si substrate. Using magnetic force and magneto-optical Kerr effect microscopy, we study the nucleation and annihilation of DWs for two different wire widths. Through scanning electron microscopy with polarization analysis, we analyze in detail the magnetization configuration of the DWs in the presence of a magnetic bead previously trapped by the DW stray field. Finally, we patterned the magnetic nanostructures directly on a polydimethylsiloxane (PDMS) substrate, and we show that the functionality of the device is completely maintained. These results pave the way to the integration of DW-based devices in a PDMS lab-on-a-chip system for magnetic bead separation. © 2012 American Institute of Physics. [<http://dx.doi.org/10.1063/1.3689009>]

I. INTRODUCTION

Domain walls (DWs) in magnetic nano-strips have been proposed as localized sources of the strong magnetic field gradient used to trap¹ and transport² individual magnetic particles. As one of the most prominent results, this technology was applied to the transport of individual viable cells labeled with magnetic beads.^{3,4} The control on the nucleation and annihilation of a series of DWs just by using external magnetic field pulses can be used to trap and release a large population of magnetic particles.

In this paper, we demonstrate the independent control over the nucleation and annihilation of arrays of traps and the integrability of this technology on a flexible polymeric membrane.

II. EXPERIMENTAL DETAILS

The devices, both on Si and on PDMS substrate, consist of a series of zig-zag nanowires of different lateral width w ranging from 200 nm to 1 μm , while the length of zig-zag segments l was maintained fixed to 2 μm [see Fig. 1(a)]. Standard e-beam writing using a double PMMA layer and lift-off process sequence was used to pattern flat permalloy (FeNi alloy, Py) nano-structures on Si substrates.

In order to fabricate magnetic nanowires on a freestanding rubber membrane, polydimethylsiloxane (PDMS) (Sylgard 184) was first dispensed on the Si substrate and spin-coated to obtain a quasi-uniform thickness layer. The PDMS precursor blend was then cured in an oven at 65° for 2 h, resulting in a rubber film thickness of nearly 500 μm . The double-layer of PMMA was subsequently spin-coated on top of the rubber substrate and covered with a 1.5-nm sputtered Au layer to avoid charge build-up effects during

the following e-beam writing step. Before final development and lift-off, the sample was soaked for a few seconds in Au etchant (Sigma Aldrich, Germany).

In the case of the PDMS substrate, at the end of the lithographic process, the flexible membrane has been simply peeled off from the Si substrate. High quality patterning of PDMS surfaces by e-beam lithography⁵ is challenging due to the surface roughness, which causes a point-by-point changing focus quality of the e-beam. In addition, wrinkles in the PMMA layer deposited on the PDMS substrate are generated during the heating process as a consequence of the different thermal expansion coefficients of the two materials. Nevertheless, in a central area of about 300 $\mu\text{m} \times 300 \mu\text{m}$ of the PDMS substrate, the surface smoothness was sufficient for a precise patterning of magnetic zig-zag nanowires.

The samples were characterized by an Agilent 5500 magnetic force microscope (MFM) and an Evico magneto-optical Kerr effect (MOKE) microscope. In the case of the samples on Si substrate, a suspension (5 μl) of Micromod Nanomag-D with diameter of 130 nm, having initial concentration of 10 mg/ml, was diluted 1:500 with MilliQ water and was dispensed on top of the magnetic nanowires after the application of a field pulse of 100 mT along the y -direction, in order to generate a magnetic trap at each corner [see Fig. 1(a)].

After drying the substrate, the magnetization configuration in the corners with trapped particles was imaged, utilizing scanning electron microscopy with polarization analysis (SEMPA).^{6,7} Due to the high surface sensitivity of SEMPA, a preparation of the sample was required in the UHV chamber of the microscope. Two different sample preparation procedures have been tried. At first, the sample surface was simply cleaned by ion milling. In addition, the surface was “dusted”, i.e., covered by a few monolayers of Fe.⁷ In both cases, identical magnetic configurations were obtained, although, in the case of dusting with Fe, a higher contrast and, thus, image quality could be attained.

^{a)}Author to whom correspondence should be addressed. Electronic mail: marco.donolato@gmail.com.

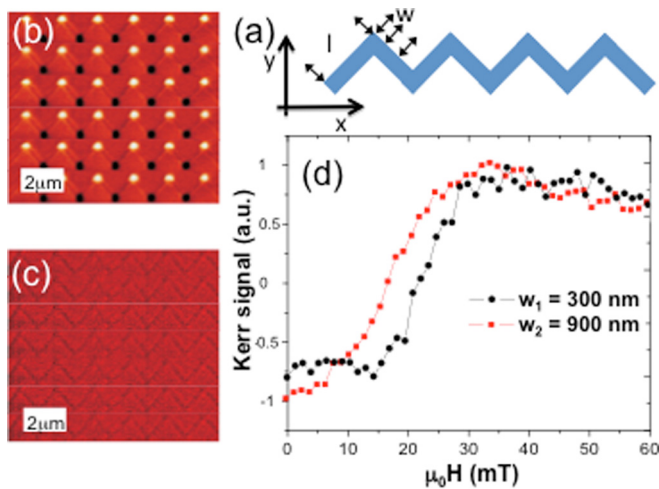


FIG. 1. (Color online) (a) Device schematic. MFM images of arrays of zig-zag wires having $w = 200$ nm after the application of field of 100 mT in the y -direction (b) and 25 mT in the x -direction (c). (d) Measured transition between the state with and without DWs for arrays of zig-zag wires of different width. The wires have been initially saturated with a field of 100 mT applied along the y -direction, and a field was then swept along the x -direction.

III. EXPERIMENTAL RESULTS

Figure 1(b) shows an MFM image of a zig-zag array ($w = 200$ nm) fabricated on Si substrate taken after applying a momentary magnetic field in the y -direction ($H_w = 100$ mT). Transverse DWs are created at every tilt, separating alternatively head-to-head and tail-to-tail-oriented domains, as evidenced by the dark and light contrast in Fig. 1(b). The DWs can be erased by applying a momentary field $H_c = 25$ mT in the x -direction, as shown in Fig. 1(c), where all DWs have been deleted.

For given wire thickness and angular aperture of the corner (90° in our case), the field strength H_c needed to erase the DWs depends on the shape anisotropy of the zig-zag segments, i.e., on the ratio between l and w . The MOKE microscope was used to experimentally characterize H_c . We

illustrate this effect for two arrays of zig-zag wires having $l = 2 \mu\text{m}$ and $w_1 = 300$ nm and $w_2 = 900$ nm, respectively.

The two samples have been initially saturated with a momentary field $H_w = 100$ mT in the y -direction in order to generate the array of DWs; after that, a second field in the x -direction has been swept from zero until the intensity at which all wires switch to the state without any DW.

For a given array, a distribution of switching fields is found with a spread of 10 mT. The MOKE signals recorded in the two cases analyzed are plotted in Fig. 1(d). The wires of width $w_2 = 900$ nm switch at H_c , that is, about 15 mT lower than that of the wires with width $w_1 = 300$ nm. This property is of particular interest in view of applications, because it provides a pathway to the independent control of the trapping and release of distinct populations of beads in different areas of the same fluidic channel.

As previously reported,³ the width of the wire provide also a means for controlling the DW micromagnetic structure, viz., the strength and spatial distribution of the magnetic field gradient. To reliably use DW-based traps, it is important to study how the presence of a magnetic bead affects the micromagnetic structure of the device.

This is shown in Fig. 2, where we compare, in detail, the illustrative cases of $w_1 = 300$ nm and $w_2 = 900$ nm. The images in the left panels (a) and (d) show the simulated trapping force acting on a magnetic bead of 130 nm of diameter in the two cases. The force has been calculated with the model explained in Ref. 4, where the simulation results were experimentally validated. In the insets of Fig. 2, the micromagnetic configurations for the two cases calculated with OOMMF⁸ are also shown.

The SEM images in the center display two of the most common cases found on the devices, i.e., a bead trapped just on the outer part of the corner in the case of the narrower wires with width w_1 [Fig. 2(b)] and beads trapped inside the corner surface for wires width w_2 [Fig. 2(e)]. The last panels on the right-hand side of Fig. 2 show the results of the SEMPA analysis with superimposed arrows plotted, representing the local direction of the magnetization as obtained

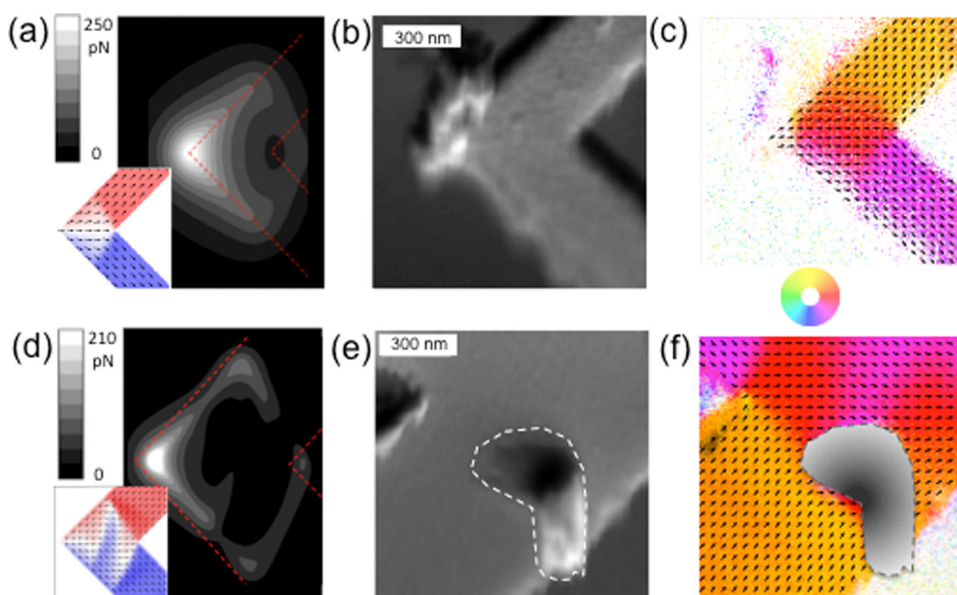


FIG. 2. (Color online) Comparison between wires having $w_1 = 300$ nm (top) and $w_2 = 900$ nm (bottom). (a) and (d) Calculated trapping force acting on a Micromod-Nanomag D of 130 nm diameter (Ref. 4) originated from the device. The insets represent the micromagnetic configuration obtained after applying a field of 100 mT along the corner bisector. (b) and (e) SEM images of two corners in the presence of a magnetic nanobead and correspondent SEMPA image (c) and (f).

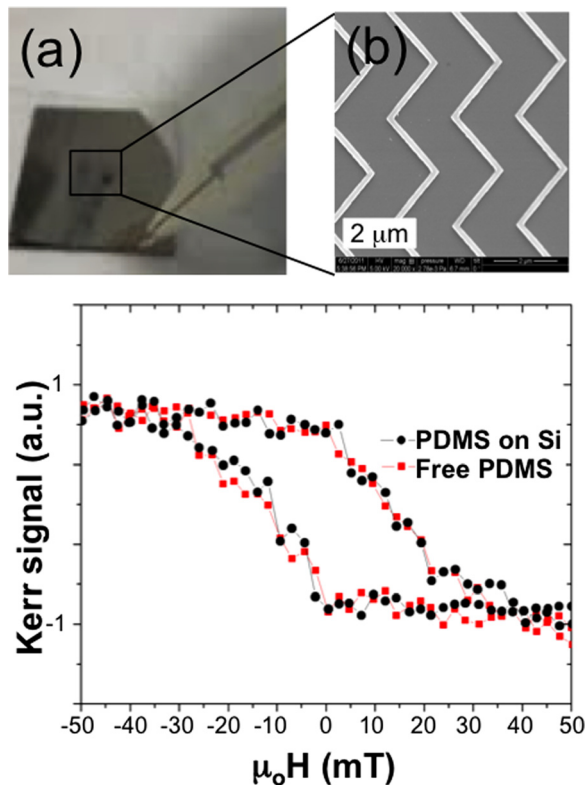


FIG. 3. (Color online) (a) PDMS substrate obtained after curing the PDMS (Sylgard 184) precursors blend. (b) Scanning electron microscope image of the permalloy wires. (c) Hysteresis loops measured before and after peeling off the PDMS membrane from the Si substrate.

from the SEMPA images analysis in accordance with the color code shown.

As previously discussed,² in the nanowires having $w_f = 300$ nm, a transverse DW is expected to form at each corner after the application of a momentary field along the corners bisector. This anticipated behavior is confirmed experimentally by the SEMPA images analysis. The trapping force, in this case, is well localized on the outer edge of each corner [Fig. 2(a)]. A careful image analysis and comparison with corners without particles reveals a weak distortion in the DW structure induced by the presence of the magnetic bead. This weak effect, due to the mutual magnetostatic interaction between the bead and the DW, was recently theoretically modeled and experimentally demonstrated.^{1,9,10}

In the case of wider magnetic wires, a marked distortion of the transverse DW magnetization structure is observed already for bare wires [see inset Fig. 2(d)]. This distorted magnetization configuration produces a less localized trapping force for the magnetic beads shown in Fig. 2(d), i.e., a less-defined position for the trapped magnetic nanoparticles on the wire surface.

This situation is experimentally analyzed in Figs. 2(e) and 2(f). In the SEMPA image, the signal arising from the area corresponding to a magnetic bead is not traceable to a defined magnetization configuration due to the non-planar surface of the bead that causes a bending of the electron trajectories around the particle itself. For this reason, in Fig. 2(f), we have masked the trapped particles in the SEMPA image to remain with only the true magnetic structure in the wire. The SEMPA image reveals that, also in this

case, the bead affects the magnetization configuration of the DW only to a minor extent [compare the inset in Fig. 2(a) with Fig. 2(f)]. In summary, for both wire widths analyzed with SEMPA, we can conclude that the DW structure is just weakly influenced by the proximity of a magnetic bead.

Finally, the same array structures patterned on a flexible PDMS substrate have been characterized with SEM and MOKE microscopy.

As previously described, the PDMS was patterned when lying on the Si substrate and finally mechanically peeled off using tweezers from the Si chip, as illustrated in the picture in Fig. 3(a). The SEM image in the inset of Fig. 3(a) shows the final device on the PDMS substrate.

To characterize the magnetic properties of the devices, we fabricate a DW injector at one end of the zig-zag structure, as previously described.² We used the high spatial resolution (500 nm) of our MOKE microscope to monitor the MOKE signal, due to the DW displacement between adjacent corners in a nanowire of width $w = 250$ nm, while sweeping a magnetic field from positive to negative saturation and back in the x-direction.

Figure 3(b) shows the comparison of the hysteresis loops measured before and after peeling off the PDMS substrate from the Si wafer. The observation of identical (within the resolution of our characterization tool) loop shapes in the two cases confirms that the magnetic properties are maintained in the freestanding device.

In conclusion, we characterized with different techniques magnetic beads traps based on transverse DWs generated in zig-zag magnetic wires both on Si and PDMS substrate. These results open the pathway to the direct integration of the DW conduits' technology on polymeric substrates for the realization of lab-on-chip magnetic separation devices.

ACKNOWLEDGMENTS

The authors acknowledge funding from the Spanish Ministry of Science and Education under Project No. MAT2009-07980 and the Basque Government through the ETORGAI Program, Project "Biodetect" No. ER-2010/00032, the Program No. PI2009-17, and fellowship No. BFI09.289.

¹M. Donolato, M. Gobbi, P. Vavassori, M. Leone, M. Cantoni, V. Metlushko, B. Ilic, M. Zhang, S. X. Wang, and R. Bertacco, *Nanotechnology* **20**, 385501 (2009).

²M. Donolato, M. Gobbi, P. Vavassori, M. Deryabina, M. F. Hansen, V. Metlushko, B. Ilic, M. Cantoni, D. Petti, S. Brivio, and R. Bertacco, *Adv. Mater.* **22**, 2706 (2010).

³M. Donolato, A. Torti, E. Sogne, N. Kostesha, M. Deryabina, P. Vavassori, M. F. Hansen, and R. Bertacco, *Lab Chip* **11**, 2976 (2011).

⁴G. Vieira, T. Henighan, A. Chen, A. J. Hauser, F. Y. Yang, J. J. Chalmers, and R. Sooryakumar, *Phys. Rev. Lett.* **103**, 128101 (2009).

⁵K. W. Rhee, L. M. Shirey, P. I. Isaacson, C. F. Korngay, W. J. Dressick, M.-S. Chen, and S. L. Brandow, *J. Vac. Sci. Technol.* **18**, 3569 (2000).

⁶R. Frösmtner, S. Hankemeier, H. P. Oepen, and J. Kirschner, *Rev. Sci. Instrum.* **82**, 033704 (2011).

⁷H. P. Oepen and H. Hopster, *Magnetic Microscopy of Nanostructures* (Springer, New York, 2005).

⁸M. J. Donahue and D. G. Porter, *OOMMF User's Guide*, Version 1.0, Interagency Report NISTIR 6376 (Gaithersburg, National Institute of Standards and Technology, 1999).

⁹M. T. Bryan, J. Dean, T. Schreffl, F. E. Thompson, J. Haycock, and D. A. Allwood, *Appl. Phys. Lett.* **96**, 192503 (2010).

¹⁰T. Klein, D. Dorroh, Y. Li, and J. P. Wang, *J. Appl. Phys.* **109**, 07D506 (2011).